International Conference KNOWLEDGE-BASED ORGANIZATION
Vol. XXX No 3 2024

ELECTROMAGNETIC FIELD MONITORING BY FIXED STATIONS IN ROMANIA: DATA PROCESSING METHODS AND OUTCOMES

Simona MICLĂUȘ*, Teodor PETRIȚA**

***"Nicolae Bălcescu" Land Forces Academy, Sibiu, Romania**
****Politehnica University, Timișoara, Romania**
simo.miclaus@gmail.com

Abstract: *Electromagnetic field (EMF) monitoring activities provide transparent information to the public interested in the safety levels of human exposure when using various radiofrequency (RF) emitting technologies. In the present work, we investigate different methods of data processing that enable relevant knowledge extraction from the databases gathered by the Romanian EMF-fixed monitoring network. Four categories of methods are proposed and illustrated by investigating the situation of electromagnetic exposure at three locations in Bucharest, during 25 months. The conducted application methods enables field level distributions and trends, time-variability on the short- and long-term basis, cumulative influence comparison and sensing of the significant changes in the environment.*

Keywords: EMF monitoring, human exposure, fixed RF sensors, national network

1. Introduction

Electromagnetic field (EMF) monitoring is an activity that have been implemented in a number of countries in the last twenty years [1]-[5]. Nevertheless, its use was implemented due to the exponential increase of radiofrequency (RF) emissions from modern communication technologies and associated health risks among the population. Safety limits, expressed as electric (E) field strength or power flux density values, are stipulated in standards for human EMF exposure [6].

In Romania, starting from 2015, the National Authority for Management and Regulation in Communications (ANCOM) implemented a network of fixed stations for broadband RF field monitoring after which some data processing results were published [7], [8]. Currently (in 2024), throughout the country, measurements are conducted exclusively outdoors, using approximately 200 broadband monitoring stations, in the frequency range 100 kHz - 7 GHz, located in >100 cities across the country. Recorded data are presented to population in the form of graphs showing average and peak E-field strength values as a function of time, while the locations are presented on the interactive map of Romania.

The current approach aimed to address the processing possibilities of raw data, originated from these sensors, to enable reliable comparisons of exposure profiles between monitoring locations, time-variability of exposures as well as their cumulative impact.

To explain and illustrate the procedures, we used data extracted from the three E-field sensors situated in Bucharest (Romania's capital) which were collecting E-field levels during 25 months, between September 1st 2018 and September 30th 2019. Descriptive

DOI: 10.2478/kbo-2024-0089

statistics, probability distribution analysis, time-series analysis, and integrative mathematics were involved to illustrate the data processing capabilities and results.

2. Materials and Methods: EMF Sensors, Data Collection and Processing

Each EMF monitoring station uses a tri-axial isotropic E-field probe models NARDA AMB 8057 and 8059 models. The probes are quad-band, with a wide band detector in the 100 kHz – 7 GHz frequency range and three band-pass capabilities in the ranges: 925-960 MHz (GSM900), 1805-1880 MHz (GSM 1800) and 2110-2170 MHz (UMTS). E-field strengths are collected every 6 minutes as a pair of average (avg) and peak values, in all four bands. The total duration of the monitoring exemplified here lasted 25 months.

Figure 1: Narda fixed stations at the three sites

Hereon, the following notations are used: B1, B5 and B8, representing the three sensors locations in Bucharest (Figure 1). The sensors B1 and B5 captured signals in the area of Politehnica University buildings, while the sensor B8 was located in the area of the main railway station. With qtsWide_Avg and qtsWide_Peak we marked the field strengths in the 100 kHz – 7 GHz range. With q2140_Avg and q2140_Peak - the UMTS cellular communication band (base stations); q1842_Avg and q1842_Peak - GSM1800 band; q942_Avg and q942_Peak - GSM900 band.

Four categories of data processing procedures were applied: a) descriptive statistics with boxplot representations as well as variance curves indicating Allan deviations calculated by measuring the differences between consecutive data samples averaged over different sampling intervals; b) integration of field levels to quantify a kind of "cumulative" response at the end of the 25 months of exposure; c) time-series analysis by applying the Poincare plots representations to express and compare the outcome that long- and short-term variability of exposures may have; d) probability distribution analysis to obtain the probability density and cumulative density functions (PDFs and CDFs, respectively) of field strength strings, consequently, extracting the specific "rules" of fitting functions.

3. Results: Exposure Levels, Time Variability, Integrative Response and Probability Distribution Analyses

Figure 2 (left and middle graphs) illustrates the temporal evolution of average and peak E-field strengths during the 25 months at three locations in the frequency range 100 kHz – 7 GHz. The average values are much higher at location B1, being gradually followed by the ones at locations B5 and B8. However, at all locations, the peak values are much closer in values in-between, whereas locations B5 and B8 present similar peak levels. Interestingly, the range of peak variations is the highest at location B8. Therefore, at location B8, we applied two methods to compare the ratios ("dynamic range") in which field levels (E_avg string and E_peak) vary in the wideband frequency range.

The first one is a two-sample test for the variance with computation of F statistic. Essentially, F statistic compares the

sciendo

International Conference KNOWLEDGE-BASED ORGANIZATION
Vol. XXX No 3 2024

ELECTROMAGNETIC FIELD MONITORING BY FIXED STATIONS IN ROMANIA: DATA PROCESSING METHODS AND OUTCOMES

Simona MICLĂUȘ*, Teodor PETRIȚA**

***"Nicolae Bălcescu" Land Forces Academy, Sibiu, Romania**
****Politehnica University, Timișoara, Romania**
simo.miclaus@gmail.com

Abstract: *Electromagnetic field (EMF) monitoring activities provide transparent information to the public interested in the safety levels of human exposure when using various radiofrequency (RF) emitting technologies. In the present work, we investigate different methods of data processing that enable relevant knowledge extraction from the databases gathered by the Romanian EMF-fixed monitoring network. Four categories of methods are proposed and illustrated by investigating the situation of electromagnetic exposure at three locations in Bucharest, during 25 months. The conducted application methods enables field level distributions and trends, time-variability on the short- and long-term basis, cumulative influence comparison and sensing of the significant changes in the environment.*

Keywords: EMF monitoring, human exposure, fixed RF sensors, national network

1. Introduction

Electromagnetic field (EMF) monitoring is an activity that have been implemented in a number of countries in the last twenty years [1]-[5]. Nevertheless, its use was implemented due to the exponential increase of radiofrequency (RF) emissions from modern communication technologies and associated health risks among the population. Safety limits, expressed as electric (E) field strength or power flux density values, are stipulated in standards for human EMF exposure [6].

In Romania, starting from 2015, the National Authority for Management and Regulation in Communications (ANCOM) implemented a network of fixed stations for broadband RF field monitoring after which some data processing results were published [7], [8]. Currently (in 2024), throughout the country, measurements are conducted exclusively outdoors, using approximately 200 broadband monitoring stations, in the frequency range 100 kHz - 7 GHz, located in >100 cities across the country. Recorded data are presented to population in the form of graphs showing average and peak E-field strength values as a function of time, while the locations are presented on the interactive map of Romania.

The current approach aimed to address the processing possibilities of raw data, originated from these sensors, to enable reliable comparisons of exposure profiles between monitoring locations, time-variability of exposures as well as their cumulative impact.

To explain and illustrate the procedures, we used data extracted from the three E-field sensors situated in Bucharest (Romania's capital) which were collecting E-field levels during 25 months, between September 1st 2018 and September 30th 2019. Descriptive

DOI: 10.2478/kbo-2024-0089

statistics, probability distribution analysis, time-series analysis, and integrative mathematics were involved to illustrate the data processing capabilities and results.

2. Materials and Methods: EMF Sensors, Data Collection and Processing

Each EMF monitoring station uses a tri-axial isotropic E-field probe models NARDA AMB 8057 and 8059 models. The probes are quad-band, with a wide band detector in the 100 kHz – 7 GHz frequency range and three band-pass capabilities in the ranges: 925-960 MHz (GSM900), 1805-1880 MHz (GSM 1800) and 2110-2170 MHz (UMTS). E-field strengths are collected every 6 minutes as a pair of average (avg) and peak values, in all four bands. The total duration of the monitoring exemplified here lasted 25 months.

Figure 1: Narda fixed stations at the three sites

Hereon, the following notations are used: B1, B5 and B8, representing the three sensors locations in Bucharest (Figure 1). The sensors B1 and B5 captured signals in the area of Politehnica University buildings, while the sensor B8 was located in the area of the main railway station. With qtsWide_Avg and qtsWide_Peak we marked the field strengths in the 100 kHz – 7 GHz range. With q2140_Avg and q2140_Peak - the UMTS cellular communication band (base stations); q1842_Avg and q1842_Peak - GSM1800 band; q942_Avg and q942_Peak - GSM900 band.

Four categories of data processing procedures were applied: a) descriptive statistics with boxplot representations as well as variance curves indicating Allan deviations calculated by measuring the differences between consecutive data samples averaged over different sampling intervals; b) integration of field levels to quantify a kind of "cumulative" response at the end of the 25 months of exposure; c) time-series analysis by applying the Poincare plots representations to express and compare the outcome that long- and short-term variability of exposures may have; d) probability distribution analysis to obtain the probability density and cumulative density functions (PDFs and CDFs, respectively) of field strength strings, consequently, extracting the specific "rules" of fitting functions.

3. Results: Exposure Levels, Time Variability, Integrative Response and Probability Distribution Analyses

Figure 2 (left and middle graphs) illustrates the temporal evolution of average and peak E-field strengths during the 25 months at three locations in the frequency range 100 kHz – 7 GHz. The average values are much higher at location B1, being gradually followed by the ones at locations B5 and B8. However, at all locations, the peak values are much closer in values in-between, whereas locations B5 and B8 present similar peak levels. Interestingly, the range of peak variations is the highest at location B8. Therefore, at location B8, we applied two methods to compare the ratios ("dynamic range") in which field levels (E_avg string and E_peak) vary in the wideband frequency range.

The first one is a two-sample test for the variance with computation of F statistic. Essentially, F statistic compares the variance between strings of data (time series) with the variance within them. At location B8 and in the wideband case, the variance of E_avg time series was 0.25, while the one of E_peak was 0.52. This led to a value F=0.48.

The second method uses Allan variance analysis [9], which is useful for evaluating and comparing the differences between the two time series. Specifically, it is used to assess the stability and fluctuations recorded in the time series, providing a measure of variation as a function of the averaging interval τ. Fig 2 (right graph) illustrates the Allan deviation curves as a function of τ. Obviously, the deviations are always higher for peaks than for average fields, indicating a larger range of variation for peak values in the studied situation.

As a comparison between all locations, Figure 4 illustrates the time series of average E-field strengths for each of the three base station (BS) emission bands. It results that each location is marked by the contribution of one or another frequency band. The largest variability of field strengths is at location B5, independently of the frequency band. Figure 4 (left graph) illustrates a comparison based on the field level distribution boxplots in the frequency range 100 kHz – 7GHz between average and peak values at three locations. From B1 to B8, a descending trend is observed, meaning that B1 location contributes to the highest exposure. The differences between mean and median of both average and peak values are the smallest at location B1. At location B5, the most significant difference between average and peak values resulted.

Figure 4 (right graph) illustrates the histograms at all locations and emphasize the narrow, but different distributions of field strengths in the time series. A similar method of illustrating dissimilarities between exposures was used to obtain Figure 5, where boxplots and histograms are represented for the narrow-bands. Besides the mean, median and quartiles, the boxplots also show the outliers. The most numerous outliers are observed at location

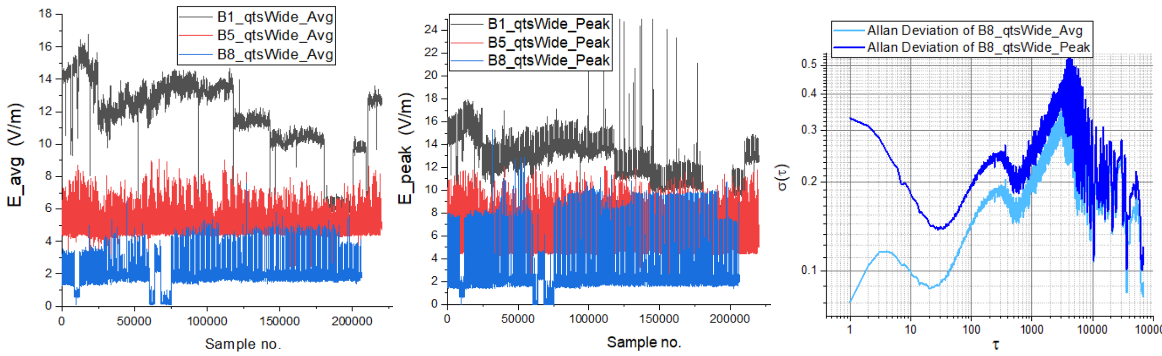

Figure 2: E-field levels (average and peak) variation along 25 months in the three locations of the Romanian capital, in the whole bandwidth 100kHz – 7GHz and Allan variance analysis in wideband

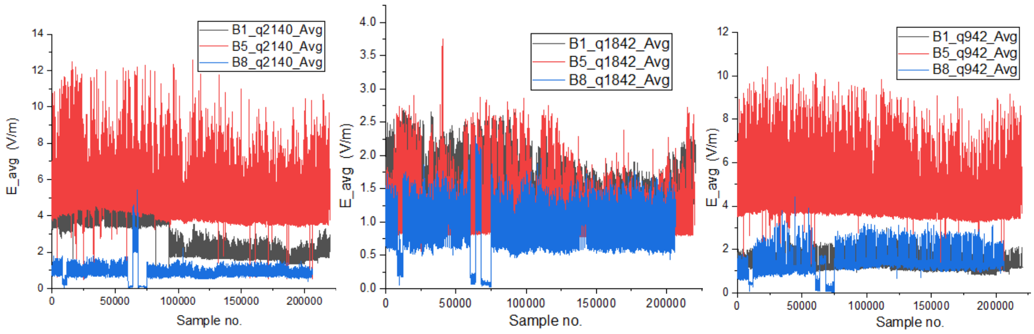

Figure 3: Average E-field levels variation along 25 months in the three locations per each narrow bandwidth of mobile communications

variance between strings of data (time series) with the variance within them. At location B8 and in the wideband case, the variance of E_avg time series was 0.25, while the one of E_peak was 0.52. This led to a value F=0.48.

The second method uses Allan variance analysis [9], which is useful for evaluating and comparing the differences between the two time series. Specifically, it is used to assess the stability and fluctuations recorded in the time series, providing a measure of variation as a function of the averaging interval τ. Fig 2 (right graph) illustrates the Allan deviation curves as a function of τ. Obviously, the deviations are always higher for peaks than for average fields, indicating a larger range of variation for peak values in the studied situation.

As a comparison between all locations, Figure 4 illustrates the time series of average E-field strengths for each of the three base station (BS) emission bands. It results that each location is marked by the contribution of one or another frequency band. The largest variability of field strengths is at location B5, independently of the frequency band. Figure 4 (left graph) illustrates a comparison based on the field level distribution boxplots in the frequency range 100 kHz – 7GHz between average and peak values at three locations. From B1 to B8, a descending trend is observed, meaning that B1 location contributes to the highest exposure. The differences between mean and median of both average and peak values are the smallest at location B1. At location B5, the most significant difference between average and peak values resulted.

Figure 4 (right graph) illustrates the histograms at all locations and emphasize the narrow, but different distributions of field strengths in the time series. A similar method of illustrating dissimilarities between exposures was used to obtain Figure 5, where boxplots and histograms are represented for the narrow-bands. Besides the mean, median and quartiles, the boxplots also show the outliers. The most numerous outliers are observed at location

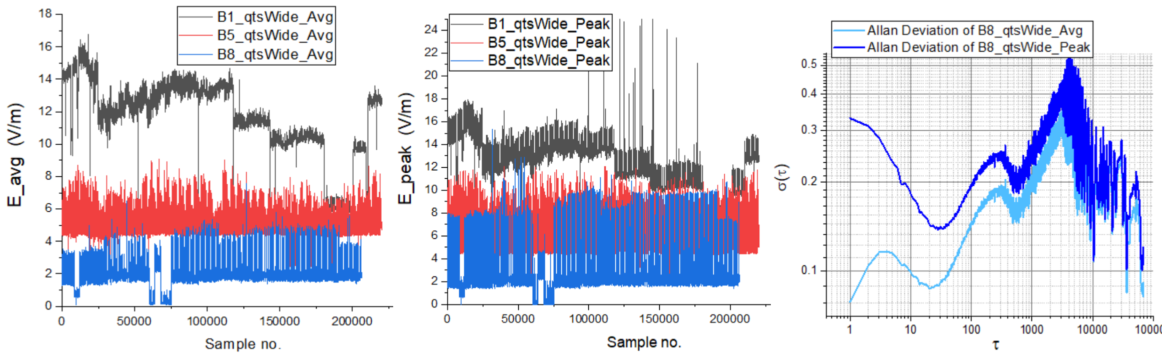

Figure 2: E-field levels (average and peak) variation along 25 months in the three locations of the Romanian capital, in the whole bandwidth 100kHz – 7GHz and Allan variance analysis in wideband

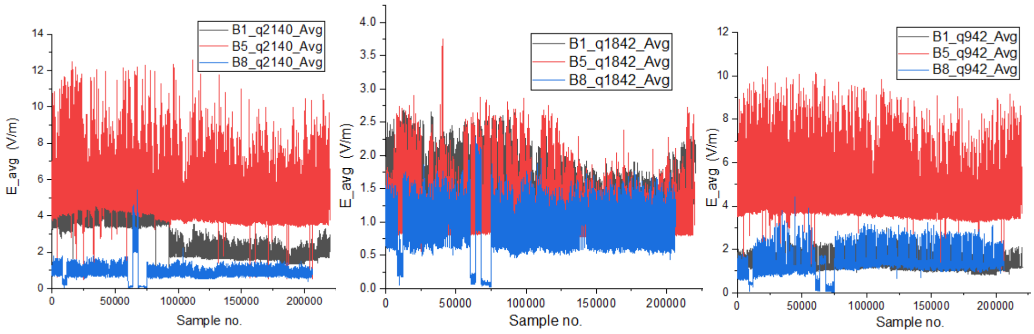

Figure 3: Average E-field levels variation along 25 months in the three locations per each narrow bandwidth of mobile communications

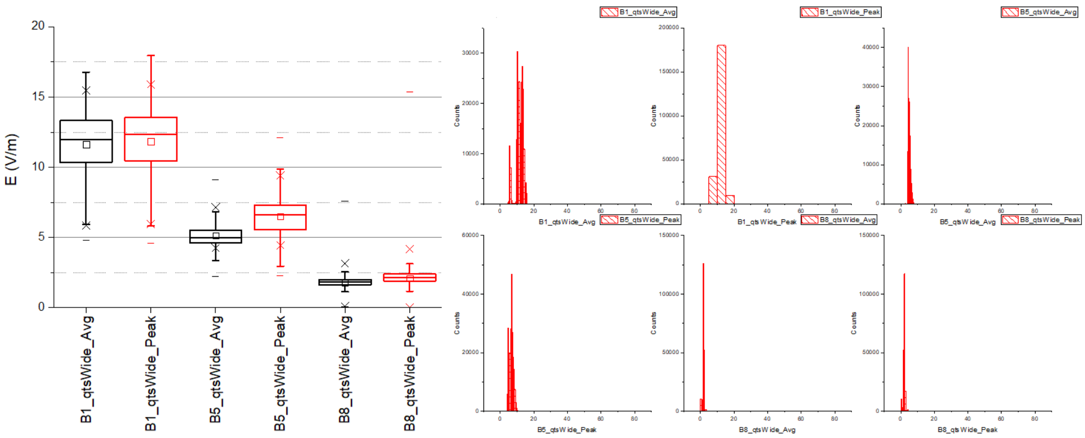

Figure 4: a) Boxplots of pair of average and peak field levels in the three locations: B1, B5 and B8; b) Field strengths distributions of average and peak values

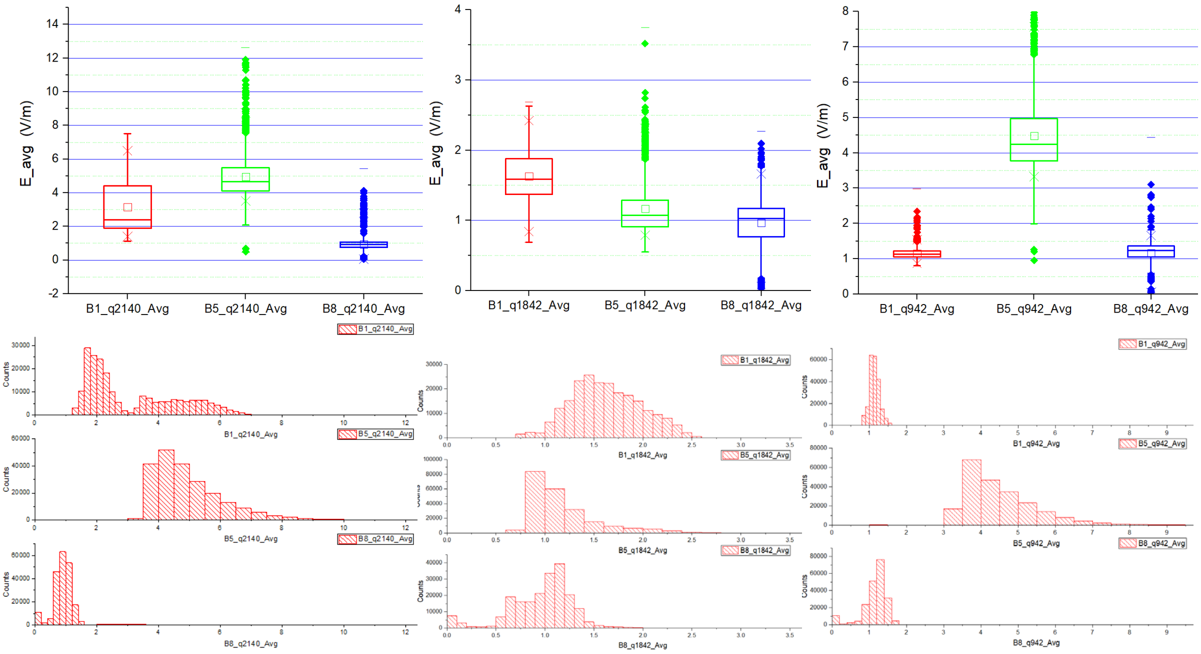

Figure 5: Upper line: boxplots of E-field levels with outliers for the three narrow bands; Lower line: histograms of field-strengths distributions in the three narrow bands

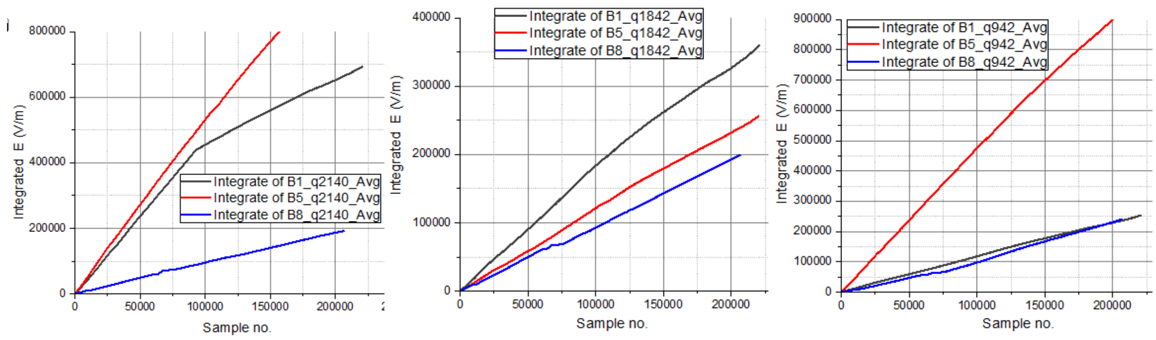

Figure 6: E-field strength accumulation in time figured by "integrated E" function: average values in the three bands of mobile communications and in all locations

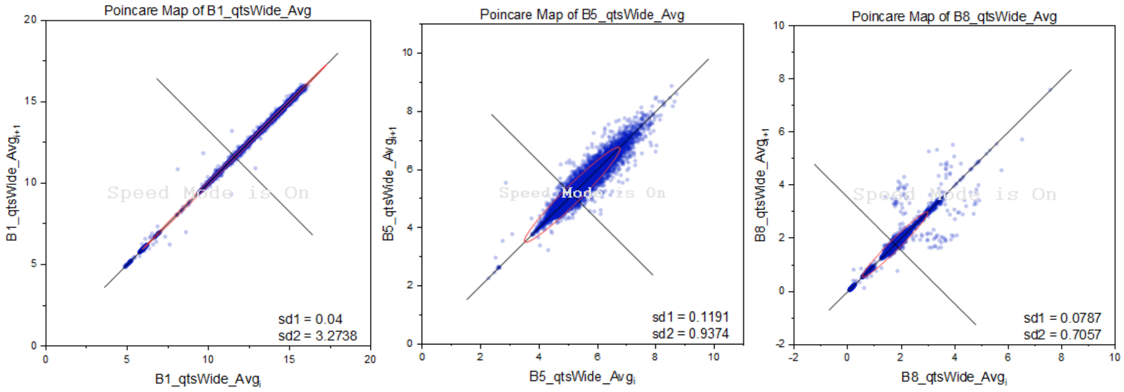

Figure 7: Poincare ellipses of the field levels in the three locations and whole bandwidth

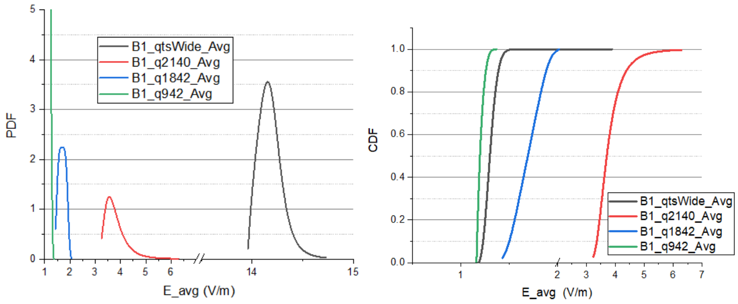

Figure 8: Probability density function (left) and Cumulative density function (right) of the field levels in location B1 for the wideband and the three narrow bands

B5, no matter which mobile communication band is measured. This observation converges to the comments given at Figure 3. Figure 6 illustrates another method enabling comparisons between exposure situations. There, we used the mathematical function of integrating the E-field level in time, along the whole time series. In this way, the amount of long-term exposure in one or another situation can be quantified. Practically, in Figure 6, the three graphs refer to each of the three mobile communications bands. For example, in UMTS, the graph in Figure 6 (left) proves that the largest rate of “incident field level accumulation” corresponds to location B5, followed by results at locations B1 and B8. However, starting from the middle of the time interval of investigation, the rate of emitted field accumulation, from an unknown reason, changed (decreased) at location B5. In the GSM900 band (Figure 6 – right), at locations B1 and B8 the rate of exposure is almost identical, so “cumulative exposure” is the same.

Time-series analysis may be approached by Poincare plots method. It allows the assessment of time variability of the exposure, both on short- and long-term. Poincaré Plot represents a graph where each point corresponds to a data point (x, y) with the x-axis representing the value at the current moment and y-axis representing the value at the successive moment. Therefore, the Poincaré Plot shows how the data are correlated between two consecutive time points. By comparing the Poincaré Plots for two groups of data, the differences in the distribution of points and structure of the time series can be observed. If the distribution or general shape of the plot differs between the two groups, this may indicate significant differences between them in terms of data variation and structure. To illustrate this method’s applicability, in Figure 7 we represented Poincare maps of average E-field strengths in the wide band for each of the three locations. The areas of the ellipses illustrate the total variability of the field levels while the ratio between the two axes (sd1 – the short one; sd2 – the long one), sd1/sd2, indicate the short- versus long-term variability. Observing the three plots in Figure 7, we conclude that the total variability of exposure is the highest at location B5 (the largest ellipse area), while the largest difference between the short- and long-term variability happens at B1 location, where sd1/sd2 is the smallest. The normality test was also applied, proving that the distribution differed from the normal. Therefore, PDF and CDF will enable asymmetries and peculiarities remarks, as shown in Figure 8 at location B1.

4. Conclusions

Present work proposes and exemplify for the first time, a series of methods destined to emphasize the possibilities of comparison between exposure profiles in space, time and frequency, based on data extracted from a fixed-station EMF monitoring system. Application of the efficient methods presented here and applied on a few datasets gathered on the servers of ANCOM, allows valuable comparisons between exposure levels in different places and situations, identification of trends and changes, short- and long-term dynamics tracing, as well as impact of new sources of EMF exposure entered into use. In the near future, the observed differences between the whole bandwidth (100 kHz - 7 GHz) and the narrow (mobile communication) bands could enable the assessment of 5G BSs emission contributions to the total exposure.

Acknowledgements
We are grateful to ANCOM Romania for providing us the data used in this work.

References List

[1] ITU-T. Monitoring of electromagnetic fields levels. *Series K*, Supplement 83. 2022. Available online: https://www.itu.int/rec/T-REC-K.83-202201-I/en.

[2] Iakovidis, S.; Apostolidis, C.; et al. Electromagnetic Fields Exposure Assessment in Europe Utilizing Publicly Available Data. *Sensors* 2022, 22 (21), 8481.

[3] Manassas, A.; Apostolidis, C.; Iakovidis, S.; Babas, D.; Samaras, T. A Study of the Long Term Changes in the Electromagnetic Environment Using Data from Continuous Monitoring Sensors in Greece. Sci Rep 2023, 13 (1), 13784.

[4] Djuric, N.; Kljajic, D.; Gavrilov, T.; Otasevic, V.; Djuric, S. The EMF Exposure Monitoring in Cellular Networks by Serbian EMF RATEL System. In: *IEEE International Symposium on Measurements & Networking* (M&N) 2022, 1-6.

[5] Aerts, S.; Vermeeren, G.; Van Den Bossche, M.; Aminzadeh, R. et al. Lessons Learned from a Distributed RF-EMF Sensor Network. *Sensors* 2022, 22 (5), 1715.

[6] International Commission on Non-Ionizing Radiation Protection (ICNIRP). Guidelines for Limiting Exposure to Time-Varying Electric, Magnetic and Electromagnetic Fields (100 KHz-300 GHz). *Health Phys*. 2020, 118.

[7] Lunca, E.; Salceanu, A. An Overview of RF-EMF Monitoring Systems and Associated Monitoring Data. In: *IEEE International Conference and Exposition on Electrical and Power Engineering (EPE)* 2016; 418-421.

[8] Ursachianu, M.; Bejenaru, O.; et. al. The Assessment of Human Exposure in Iasi-City Using Data Provided by The National Autonomous RF-EMF Monitoring System throughout 2020. In: *IEEE International Conference on Electromechanical and Energy Systems (SIELMEN)* 2021; 225-230.

[9] Allan D. W. Statistics of atomic frequency standards. In: *Proceedings of the IEEE*, 1996, 54(2), 221-230.